Phase Coexistence in Gallium Nanoparticles Controlled by Electron Excitation

S. Pochon, K. F. MacDonald, R. J. Knize,* and N. I. Zheludev†

School of Physics and Astronomy, University of Southampton, SO17 1BJ, United Kingdom

(Received 7 November 2003; published 9 April 2004)

In gallium nanoparticles 100 nm in diameter grown on the tip of an optical fiber from an atomic beam we observed equilibrium coexistence of γ, β, and liquid structural phases that can be controlled by e-beam excitation in a highly reversible and reproducible fashion. With 2 keV electrons only 1 pJ of excitation energy per nanoparticle is needed to exercise control, with the equilibrium phase achieved in less than a few tenths of a microsecond. The transformations between coexisting phases are accompanied by a continuous change in the nanoparticle film's reflectivity.

DOI: 10.1103/PhysRevLett.92.145702 PACS numbers: 64.70.Nd, 78.67.–n

We report that *controllable*, *continuous*, and *reversible* phase coexistence of different crystalline and disordered phases can be achieved in gallium nanoparticles under electron-beam excitation. Our study of electron-beam excitation of gallium nanoparticles is motivated in part by a desire to understand the exciting physics of phase equilibria in metallic nanoparticles and clusters [1–3] whose thermodynamic properties can be radically different from those of the bulk [4]. In addition, the increasing interest in the properties of metallic nanoparticles is driven by the role that they are expected to play in future highly integrated photonic devices as the active elements of waveguiding [5] and switching [6] structures.

Electron beams provide a very fine tool to study small particles, not only for imaging, but also for preparing excited states of matter. For instance, delicate stimulation under an electron microscope has allowed the observation of structural instabilities in very small metallic clusters [7,8] and revealed the complexity of nanoparticle plasmonic excitation stimulated by the electron beam [9]. Excitation of gallium nanoparticles with an electron beam is a multistage process, resulting in heating through the loss of kinetic energy of bombarding electrons and excitation of the electronic substructure of gallium which has elements of covalent bonding. The energy of the 2 keV electrons used in our experiments is not sufficient to damage the nanoparticles' material by direct displacement of gallium atoms, but it is above the $2p$ and $2s$ electron removal thresholds and is therefore sufficient for multiple ionization of Ga atoms by electron impact: $e + \mathrm{Ga} \rightarrow e + \mathrm{Ga}^{n+} + ne$ up to $n = 4$. The single electron ionization cross section is about $\sigma_1 \approx 0.7 \times 10^{-16}\ \mathrm{cm}^2$ while the total higher order contribution is about $\sigma_{2+3+4} \approx 0.2 \times 10^{-16}\ \mathrm{cm}^2$ [10]. The 2 keV electrons provide relatively even excitation of the nanoparticle volume as the first ionization absorption depth in solid Ga is about 50 nm: $r = 2.76 \times 10^{-2} A E_0^{1.67}/\rho Z^{0.89}$, where $A = 69.723$ is the atomic mass, E_0 is the accelerating voltage (keV), $\rho = 5.91\ \mathrm{g\,cm}^{-3}$ is the density, and $Z = 31$ is the atomic number of the gallium target [11]. The resultant secondary electrons and holes created in the Auger process cause further ionization, generating an avalanche of electrons which develops and decays on the subpicosecond time scale, from the initial electron impact, creating heat, a high density of electron-hole pairs, and plasmon excitations which can affect the phase equilibrium of the nanoparticle.

As a playfield to study phase equilibria, gallium is a unique metal in that ten structural solid phases are known. Five phases (α, β, γ, δ, ε) can exist at low pressure [12]. We studied electron-beam induced structural transformations in Ga nanoparticles on the tip of a silica optical fiber. The stimulated structural transformations were detected optically by monitoring the nanoparticle film reflectivity through the fiber. Because of the very significant differences in the electronic and optical properties of the various phases of gallium [13], optical measurements provide a very sensitive tool for detecting nanoparticle phase composition. A schematic of the apparatus is shown in Fig. 1. Nanoparticles were grown using the light-assisted deposition technique [14]. This technique yielded particles of relatively narrow size distribution with diameters of about 100 nm. The fiber core

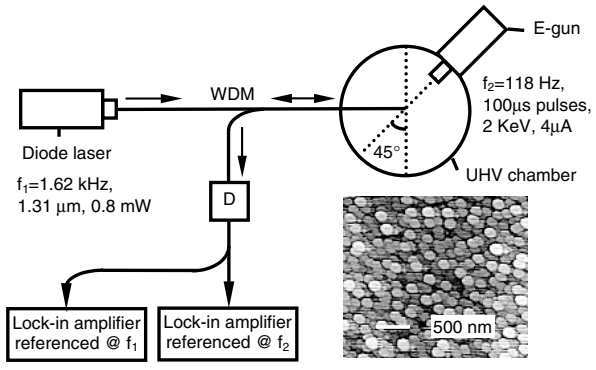

FIG. 1. Schematic diagram of the apparatus. The inset shows an atomic force microscope (AFM) image of gallium nanoparticles located on the core area of a fiber (the particles are actually a factor of 1.6 smaller than they appear in the picture due to the microscope's instrumental function).

($9\ \mu$m in diameter) contained approximately 6×10^3 nanoparticles. All experiments were conducted in a vacuum chamber evacuated to 10^{-6} mbar. In the chamber, the fiber tip supporting the nanoparticles was attached to the coldfinger of a nitrogen flow cryostat. After the experiments, the fiber was removed from the vacuum chamber and examined with an atomic force microscope.

The nanoparticles were stimulated by a 2 keV electron beam focused to a spot about 100 μm in diameter to encompass all of the nanoparticles on the fiber core. The electron gun current of 4 μA used in our experiments corresponded to an electron-beam intensity at the fiber core of approximately 100 W cm^{-2}. The e-beam was modulated to give 100 μs pulses with a repetition rate of 118 Hz, providing an average power of about 120 pW per nanoparticle, or a total energy of 1 pJ per pulse per nanoparticle. To monitor the film's reflectivity, we used a diode laser operating at 1.31 μm with a power of 800 μW, modulated at a frequency of 1.62 kHz. The intensity of reflected light was detected with two phase-sensitive amplifiers. One amplifier was locked at the frequency of electron-beam modulation, to detect electron-beam induced effects, the other was locked at the probe beam modulation frequency, to monitor variations of the sample reflectivity. Our experiments were performed in the temperature range from 80 to 250 K. The temperature of the coldfinger was measured with an absolute accuracy better that 0.5 K, but was somewhat lower than the actual temperature of the nanoparticles at the fiber tip due to electron beam and laser heating effects. The temperature scale presented here in the experimental graphs takes this into account and was calibrated using the melting temperature of the gallium nanoparticles.

Structural transformations were observed by monitoring the nanoparticle film reflectivity and electron-beam induced reflectivity changes during heating-cooling cycles. Reflectivity recorded during the first heating-cooling cycle after growth is shown in Fig. 2(a) (bold curve). The reflectivity showed an increase during heating at about 120 K and a much larger increase which begins around 230 K, with a total reflectivity change of about 1.7%. It remains high during cooling down to about 145 K, where it rapidly decreases to form an incomplete hysteresis loop about 100 K wide. In the next heating-cooling cycle (faint curve), the hysteresis loop remains very wide, but becomes much more shallow (about 0.75% total change) and nearly complete.

The modulated electron beam induces an increase in the optical reflectivity as shown in Fig. 2(b) for the first heating-cooling cycle. A large peak is observed at 231 K and a smaller peak at 248 K. At temperatures above the second peak, the electron-beam induced signal becomes negative (reflectivity decreases), and remains negative during cooling down to about 180 K. On the cooling part of the curve, a peak is seen at 120 K, corresponding

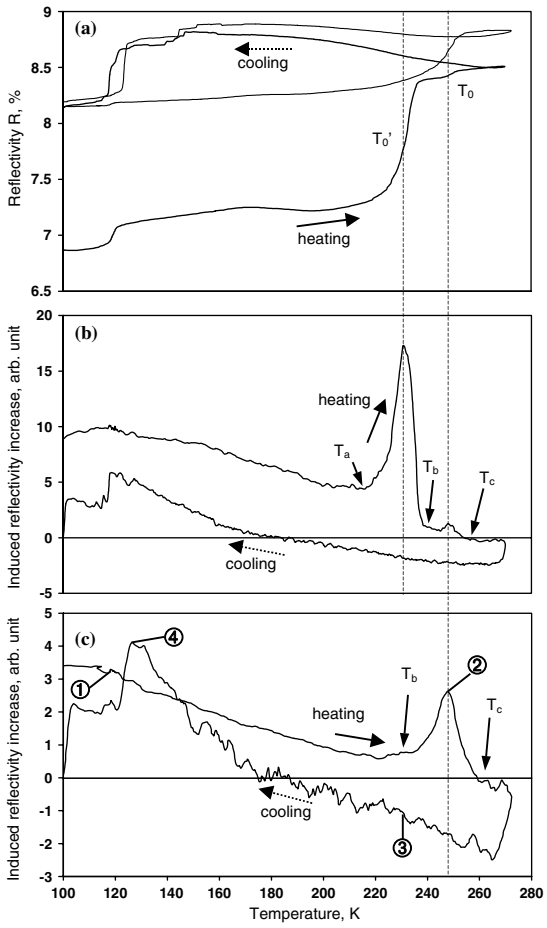

FIG. 2. Temperature dependences of (a) reflectivity R, (b) electron-beam induced reflectivity change during the first temperature scan, and (c) electron-beam induced reflectivity change for following scans.

to the reflectivity drop. The second and subsequent temperature scans show that the first rising temperature peak disappears and the second peak (at 248 K) increases [Fig. 2(c)]. We also performed measurements of the transient dynamics of the induced reflectivity change with 2 μs electron pulses. Reflectivity was then monitored using an amplified photodetector and real time digital scope. We observed essentially nonexponential reflectivity relaxation and an increase in the relaxation time of the response at temperatures where the nonlinear response is peaking (Fig. 3).

We argue that our experiment reveals a reversible electron-beam induced structural transformation in nanoparticles in the form of a controlled dynamic coexistence between different structural forms. The surface of a particle, where atoms have fewer nearest neighbors than internal atoms, acts as a boundary at which transformation processes start. To detail this process further, we shall consider a nanoparticle with a core consisting of a certain structural phase covered by a ''shell'' of different composition. Comparison with energy-dispersive

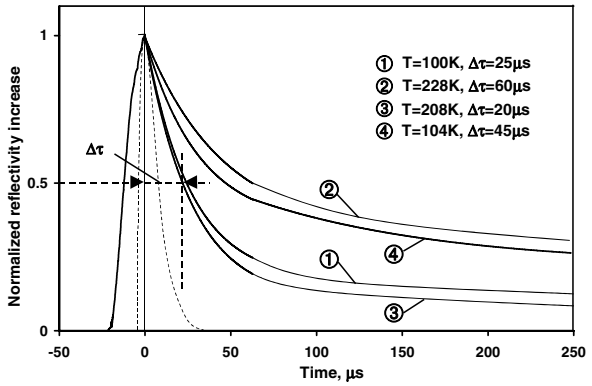

FIG. 3. Normalized transient reflectivity response of a gallium nanoparticle film to 2 μs electron beam pulses for the four numbered positions shown in Fig. 2(c). Characteristic relaxation times ($\Delta\tau$) are measured at half maximum. The dotted curve shows the response of the detector system to a 3 ns optical pulse.

x-ray diffraction studies of gallium nanoparticles [15] suggests that the low-temperature phase is γ gallium, with a bulk melting temperature of 238 K, and that the intermediate phase is β gallium, with a bulk melting temperature of 257 K. The melting temperatures in nanoparticles are depressed in comparison with those of the bulk by $\delta T = K/d$, where K is a function of the metastable phase's surface tension, molar volume, bulk melting temperature, and latent heat, and d is the nanoparticle diameter. For the β phase $K = 600$ K nm [16]. This gives the β-gallium nanoparticles a melting temperature of about 251 K. In the simplest case of a phase transition to the melt in the nanoparticle, the electron-beam induced behavior should be analogous to the temperature-driven "surface melting" effect that has been seen in lead nanoparticles [17] and found to be thermodynamically reversible within a narrow temperature range [18]. In reality, the situation is complicated by the presence of two steps in the first reflectivity dependence [Fig. 2(a)] at T_0' and T_0 (bold curve). Assuming the same melting point depression coefficient for all phases involved, the difference between the melting points of the γ and β phases is about 19 K which is close to the 17 K difference observed between the first and second peaks on Fig. 2(b), indicating that T_0' is the melting temperature of the γ phase. In a multiphase nanoparticle, there are two possible scenarios, either the nanoparticles first undergo a transition from one solid phase to another at T_0', and then from that phase to the liquid at T_0, or different solid phases with different melting points initially coexist in nanoparticles at low temperature. In the presence of electron excitation, the phase equilibrium will be determined by both temperature and electron-beam intensity.

In the first transition scenario, the influence of excitation on the equilibrium becomes apparent in the changing reflectivity of the film at a temperature T_a below T_0' [see Fig. 2(b)]. With increasing temperature or level of excitation, the β-gallium surface layers' thickness increases until the transformation of the γ-gallium core to the "surface" phase is completed. When, at T_b, the core of the particle is fully consumed by the β phase, the nanoparticle becomes stable against a return to the γ phase because this would require the creation of a nucleation center. However, if the temperature or level of electronic excitation is reduced *before* the transformation to the new phase is complete, i.e., while a nucleus of the old core phase is still present, the transformation is reversed and the skin layer shrinks to an appropriate equilibrium position. Thus, reversibility is provided in the temperature range between T_a and T_b. This whole process is then replicated between T_b and T_c, around the next transition temperature T_0 between the β and liquid phases [see Fig. 4(a)]. It then appears that on cooling, the nanoparticles return to the β phase but the γ phase is not present anymore. This is evident from the shallower reflectivity hysteresis. During the second and following temperature cycles, the nanoparticles in the β phase only go through the second stage of transformation, as presented in Fig. 4(c).

In the second scenario, the γ and β phases coexist in gallium nanoparticles after their formation on the substrate from the atomic beam. The first temperature cycle then shows consecutive melting of the γ component at T_0' and of the β component at T_0, as presented in Fig. 4(b). It is not, however, possible to distinguish between the two transformation scenarios outlined above on the evidence

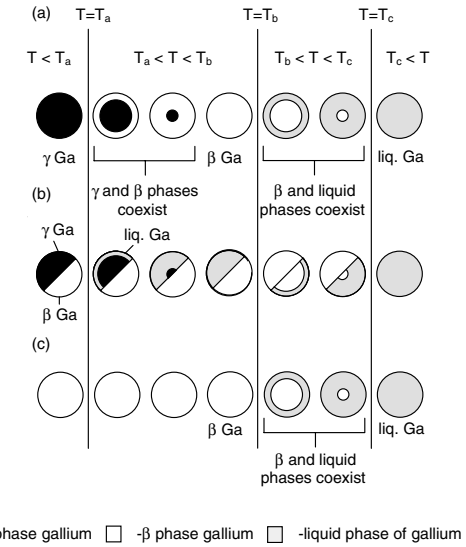

FIG. 4. Schematic representation of possible phase coexistence scenarios in gallium nanoparticles. (a) Solid-solid-liquid transition (first temperature cycle), (b) coexistence of different solid phases and two overlapping solid-liquid transitions (alternative scenario for the first temperature cycle), and (c) solid-liquid transition (following temperature cycles).

of the reflectivity data available to us, and this shall be left for further investigations. It is also possible that the two-step process observed during the first temperature cycle results from the coexistence of nanoparticles of different ground states immediately after growth. Whatever the phase composition of the particles, the longer relaxation observed around the peaks in the nonlinear response indicates an increase in the time needed for the phase boundary to travel across the increasingly thick shell layer.

The strength of the phase coexistence concept is supported by our calculations of the optical properties of gallium nanoparticle films on a dielectric substrate using a recently developed effective-medium model for densely packed nanoshells [19]. For the purposes of our calculations, the dielectric constants of β and γ gallium, which are much closer to those of a free-electron metal than those of the α phase, were estimated by using the damping constant in Drude's free-electron model as a fitting parameter to produce the nanoparticle film reflectivity levels shown in Fig. 2(a). These calculations confirmed that the presence on each nanoparticle of a shell just a few nanometers thick in a phase different from the core can produce a change in reflectivity sufficient to explain our experimental data.

A thermally activated transition due to electron-beam-induced heating can explain certain characteristics of the effect. For instance, by assuming a local electron-induced temperature increase of 4 K, one can derive a good facsimile of the experimental peaks in induced reflectivity increase at T_0' and T_0 from the reflectivity data in Fig. 2(a). However, there are serious discrepancies between the results of this thermal model and the experimental results, primarily at temperatures more than a few degrees below the peaks, where the observed effect is larger than predicted by the thermal model. This suggests that another, temperature-independent, nonthermal excitation mechanism is also contributing to the effect. This mechanism may be especially important for β gallium because its structure contains covalent bonds [13]. As with the excitation mechanism in e-beam pumped semiconductor lasers, electron-beam excitation in gallium results in bonding-antibonding transitions, which destabilize the crystalline structure [20]. This mechanism should be especially effective in nanoparticles as the electron-beam penetration depth in gallium is of the order of their diameter. An "inclusion" of a new phase is thus created, changing the optical properties of the "host" phase at temperatures far below its transition point and shifting the phase equilibrium, promoting the formation of a thicker layer of the new phase without any increase in temperature [21].

In conclusion, we observed equilibrium coexistence of different structural phases in gallium nanoparticles a few tens of nanometers in diameter that can be controlled by e-beam excitation in a highly reversible and reproducible fashion. We expect that such transitions may also be seen in much smaller particles where it is possible that, depending on size and geometry, they could adopt an unknown structural configuration that is unstable or unavailable in the bulk [4,15], and that phase transitions will occur through sequential melting of relatively stable shells of atoms at the particle surface [22], providing exciting prospects for the extension of this work.

The authors acknowledge the financial support of the EPSRC (U.K.).

*On sabbatical leave from the U.S. Air Force Academy, Colorado Springs, Colorado 80840, USA.
†Electronic address: n.i.zheludev@soton.ac.uk

[1] B. M. Smirnov, Phys. Scr. **50**, 427 (1994).
[2] R. S. Berry, J. Jellinek, and G. Natanson, Phys. Rev. A **30**, 919 (1984).
[3] R. S. Berry and B. M. Smirnov, J. Chem. Phys. **113**, 728 (2000).
[4] G. A. Breaux, R. C. Benirschke, T. Sugai, B. S. Kinnear, and M. F. Jarrold, Phys. Rev. Lett. **91**, 215508 (2003).
[5] J. R. Krenn *et al.*, Phys. Rev. Lett. **82**, 2590 (1999).
[6] N. I. Zheludev, Contemp. Phys. **43**, 365 (2002).
[7] P. Williams, Appl. Phys. Lett. **50**, 1760 (1987).
[8] S. Iijima and T. Ichihashi, Phys. Rev. Lett. **56**, 616 (1986).
[9] N. Yamamoto, K. Araya, and F. J. Garcia de Abajo, Phys. Rev. B **64**, 205419 (2001).
[10] C. J. Patton, K. O. Lozhkin, M. B. Shah, J. Geddes, and H. B. Gilbody, J. Phys. B **29**, 1409 (1996).
[11] K. Kanaya and S. Okayama, J. Phys. D **5**, 43 (1972).
[12] A. Defrain, J. Chim. Phys. **74**, 851 (1977).
[13] M. Bernasconi, G. L. Chiarotti, and E. Tosatti, Phys. Rev. B **52**, 9988 (1995).
[14] K. F. MacDonald, V. A. Fedotov, S. Pochon, K. J. Ross, G. C. Stevens, N. I. Zheludev, W. S. Brocklesby, and V. I. Emel'yanov, Appl. Phys. Lett. **80**, 1643 (2002).
[15] A. Di Cicco, Phys. Rev. Lett. **81**, 2942 (1998).
[16] E. V. Charnaya, C. Tien, K. J. Lin, and Y. A. Kumzerov, J. Phys. Condens. Matter **10**, 7273 (1998).
[17] R. Garrigos, P. Cheyssac, and R. Kofman, Z. Phys. D **12**, 497 (1989).
[18] K. F. Peters, Y. W. Chung, and J. B. Cohen, Appl. Phys. Lett. **71**, 2391 (1997).
[19] V. A. Fedotov, V. I. Emel'yanov, K. F. MacDonald, and N. I. Zheludev, J. Opt. A **6**, 155 (2003).
[20] Y. Siegal, E. N. Glezer, L. Huang, and E. Mazur, Annu. Rev. Mater. Sci. **25**, 223 (1995).
[21] K. F. MacDonald, V. A. Fedotov, R. W. Eason, N. I. Zheludev, A. V. Rode, B. Luther-Davies, and V. I. Emel'yanov, J. Opt. Soc. Am. B **18**, 331 (2001).
[22] M. Y. Efremov, F. Schiettekatte, M. Zhang, E. A. Olson, A. T. Kwan, R. S. Berry, and L. H. Allen, Phys. Rev. Lett. **85**, 3560 (2000).